Polymer Chemistry

PAPER

Cite this: *Polym. Chem.*, 2015, **6**, 6358

Liquid crystalline side-chain triblock copolymers consisting of a nematic central subblock edged by photochromic azobenzene-containing fragments: their synthesis, structure and photooptical behaviour†

N. I. Boiko,*[a] M. A. Bugakov,[a] E. V. Chernikova,[a] A. A. Piryazev,[b] Ya. I. Odarchenko,‡[b] D. A. Ivanov[b,c] and V. P. Shibaev[a]

Received 15th April 2015,
Accepted 15th July 2015

DOI: 10.1039/c5py00555h

www.rsc.org/polymers

For the first time, symmetrical photosensitive fully liquid crystalline side chain triblock copolymers (pAzo-*b*-pPhM-*b*-pAzo) and random copolymers (pAzo-*ran*-pPhM) with nematogenic phenyl benzoate (PhM) and photosensitive smectogenic azobenzene containing groups (Azo) were synthesized by the combination of RAFT polymerization and subsequent chemical modification. The central block of synthesized photochromic block copolymers contains 80 PhM groups, while the length of "peripheral" blocks includes 4 or 10 Azo units. The microphase separation structure is observed in the block copolymer when the length of a subblock with Azo groups reaches ten monomeric units. The influence of photochromic polymers' molecular architecture (homopolymer, block copolymer and random copolymer) on the photochemical and photoorientation processes induced by light in their amorphous films has been revealed. The optical anisotropy induced in block copolymer films by illumination with linearly polarized 546 nm light was studied and the results were compared with those of the Azo homopolymer and of a random copolymer with a similar composition. It was found that practically only Azo groups are included in the process of photoinduced orientation in films of block copolymers, whereas the orientational cooperative effect of both azobenzene chromophore and phenyl benzoate mesogenic groups is observed in the case of a random copolymer.

Introduction

In the last few decades, the interest in the design of and research into the "smart" materials regulated at molecular and supramolecular levels under external fields (*e.g.*, electromagnetic, mechanical, thermal fields *etc.*) has been growing considerably. Liquid crystalline (LC) azobenzene-containing polymers belong to such materials capable of providing a fast response to the light action through a reversible photoinduced *E–Z* isomerization of the azobenzene (Azo) chromophore, accompanied by large changes of its molecular size, shape, and polarity.[1–3] These structural changes may essentially influence the wettability,[4,5] phase transitions,[6–9] thin film contraction,[10–17] and surface modification[18–20] of polymers. Upon irradiation by linearly polarized light the Azo chromophores are known to orient preferentially in the direction perpendicular to the polarization plane of the excitation light (Weigert effect[21]). This behavior is due to the repeated cycles *E–Z–E* isomerization is induced by the action of light and is accompanied by rotational diffusion of the chromophore. Photoorientation processes result in the appearance of photoinduced optical anisotropy (birefringence and dichroism) which makes this type of photoresponsive materials interesting for many applications in the field of photonics and holography.[22–32]

Incorporation of Azo-containing segments into block copolymers (BCPs) in which the Azo moiety plays the role of a mesogen and a photosensitive chromophore is of considerable interest. The combination of microphase-separated

[a]*Faculty of Chemistry, Moscow State University, Leninskie Gory, Moscow, 119991, Russia. E-mail: boiko2@mail.ru*
[b]*Faculty of Fundamental Physical and Chemical Engineering, Lomonosov Moscow State University (MSU), GSP-1, Leninskie Gory - 1, 119991 Moscow, Russia*
[c]*Institut de Sciences des Matériaux de Mulhouse, CNRS UMR 7361, 15, rue Jean Starcky, F-68057 Mulhouse, France*

† Electronic supplementary information (ESI) available: ^{1}H and ^{13}C NMR spectra, GPC, POM, DSC, WAXS, and UV-visible spectroscopy data. See DOI: 10.1039/c5py00555h

‡ Present address: School of Biological Sciences, Royal Holloway, University of London, Egham, Surrey, TW20 0EX, UK.

morphologies (*e.g.*, lamellae, spheres, cylinders) inherent to block copolymers with the anisotropy and photosensitivity of an azobenzene moiety opens up the possibility of designing new light driven materials with optically controlled physical properties on various scales. These polymer materials are promising for different technical applications, namely photonic memories, optical switching, volume holographic recording, surface-relief grating (SRG) formation *etc*.

A large number of Azo-containing LC block copolymers of different molecular architectures, such as side-chain polymers,[33–39] main-chain polymers,[40,41] and dendritic polymers[42–46] with covalently, ionically or hydrogen attached mesogenic groups have been synthesized and described. The majority of publications devoted to Azo-containing LC di- and triblock copolymers focus on the side-chain rod-coil block copolymers composed of both LC and amorphous blocks. Such block copolymers have been synthesized, as a rule, by atom transfer radical polymerization (ATRP) or reversible addition–fragmentation chain transfer polymerization (RAFT).

For example, it has been shown[47] that an LC diblock copolymer consisting of polystyrene and Azo-containing subblocks is able to alter the orientation of the microphase separated (MPS) cylinder structure of coiled polystyrene microdomains periodically dispersed in the Azo LC matrix in response to linearly polarized light (LPL). Photocontrolled microphase separation in 2D has been demonstrated for a monolayer of triblock copolymer composed of poly(ethylene glycol) and azobenzene-containing polymethacrylate blocks.[34] Nagano *et al.* reported time-resolved *in situ* measurements of the photoinduced alignment changes of both smectic LC Azo-containing layers and coiled poly(butyl methacrylate) cylindrical microdomains in a block copolymer array by X-ray scattering.[48]

On the other hand, there are only a few papers dealing with Azo-containing side-chain diblock copolymers composed solely of LC blocks[49–51] (*i.e.*, so-called fully liquid crystalline block copolymers) that form various types of mesophases in the individual state. Y. Zhao *et al.* presented the first observation of photoinduced microphase separation in a BCP composed of two side-chain LC polymers[50] due to the shape incompatibility of *cis* isomers of Azo moieties with an ordered LC phase. Azo-containing diblock copolymers that are composed of two different side-chain LC polymers were synthesized by RAFT polymerization in ref. 51. It was shown that the photoorientational cooperative effects can be effective even in the microphase-separated samples due to the interaction of the two different mesogens *via* the interface. The obtained data demonstrate the ability of such block copolymers to rearrange their microphase-separated supramolecular structures under the action of electromagnetic fields.

Thus, to our knowledge, no systematic investigations into the photochromic fully LC block copolymers has been reported. Meanwhile, the synthesis of such block copolymers opens broad potentialities for the molecular design of new generation polymers that are composed of chemically distinct LC side-chain subblocks with their own functionality and properties. Investigations of the novel and well-defined fully LC block copolymers are necessary to understand the structure/property relationships and are important from the viewpoint of the fundamental understanding and practical applications of these unique materials in photonics and optoelectronics.

In the light of these considerations, here we report on the synthesis by RAFT polymerization and characterization of a novel family of symmetrical fully LC acrylic side-chain triblock copolymers (Fig. 1). The central subblock of synthesized block copolymers contains 80 phenyl benzoate mesogenic groups, while the length of "peripheral" terminal subblocks includes 4 or 10 azobenzene units.

Parallel to the synthesis of the block copolymers we also obtained a random copolymer consisting of the same monomer units. The latter was prepared in order to determine the effect of the molecular structure of photochromic copolymers on their physical–chemical properties. We also investigated "basic" homopolymers and block copolymers containing methylaniline groups using azocoupling reaction, as standards of comparison.

Of special interest is a comparative photooptical study of the triple block copolymers and statistical copolymers consisting of the same chemical components. It is well-known that the statistical azobenzene containing copolymers display a cooperative orientational effect[24,25] under the light illumination that does not allow us to control the optical properties of individual components. However, the situation associated with triblock copolymers is not clear. We wanted to reveal a possibility of controlling the photooptical behaviour of only photochromic individual subblocks with their specific properties keeping the properties of the second component unchangeable.

One of the reasons for the selection of Azo chromophores was the fact that the polymers containing these chromophores exhibit interesting properties, such as photo-induced anisotropy,[49,52–54] SRG formation[18,19] and non-linear optical properties.[55–57]

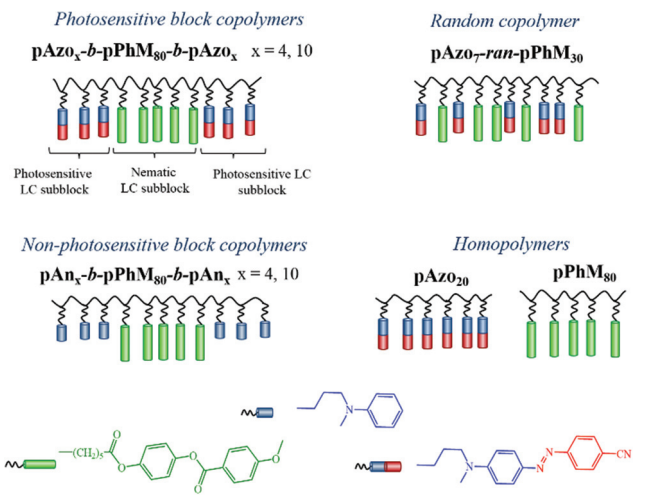

Fig. 1 Chemical structures of the synthesized acrylic polymers.

Experimental section

Materials

Toluene, DMF, and ethyl acetate were dried over molecular sieves and distilled; THF and diethyl and petroleum ethers were distilled over KOH; anisole was boiled over sodium with benzophenone until the appearance of blue color and then distilled. Triethylamine and *N*-methylaniline were distilled under reduced pressure. An Ambersep 900 (the OH form) anion-exchange resin was purchased from Acros and dried at 110 °C in a vacuum before use. AIBN was recrystallized from anhydrous methanol before use. All other reagents were used as received except when specially mentioned.

Syntheses of the monomers and polymers

3-[Methyl(phenyl)amino]propyl acrylate (compound A in Scheme 1) and the transfer agent *S*,*S*′-bis(methyl-2-isobutyrate) trithiocarbonate (BMITC in Scheme 1) were synthesized as described in ref. 58, 59. 4-(6-Acryloyloxycapryloyloxyphenyl)-4-methoxybenzoate (monomer PhM in Scheme 1) was synthesized and purified according to the literature method.[60]

The synthetic details of triblock copolymers, ^{1}H NMR spectra of the intermediate products, and the monomers and polymers are given in the ESI (Fig. S1–S7†). The main characteristics of the synthesized polymers are given in the Results and discussion section below.

Characterization

The molecular mass characteristics of the polymers were studied by SEC in THF using a chromatograph equipped with a Phenomenex 19 mm × 300 mm semi-preparative column packed with ultrastyragel with a pore size of 1000 Å and refractometric (Waters R-410) and UV-detectors. Molecular masses were calculated relative to PS standards. ^{1}H NMR spectra of the polymers in the form of 3% solutions in $CDCl_3$ were recorded on a Bruker DRX500 instrument.

The polarizing optical microscope (POM) investigations were performed using a LOMO P-112 polarizing microscope equipped with a Mettler TA-400 heating stage.

The phase transition temperatures of the polymers were studied by differential scanning calorimetry (DSC) with a PerkinElmer DSC-7 thermal analyzer with a scanning rate of 10 K min^{-1}. Samples were prepared as 10–20 mg pellets. Samples were first heated above isotropic melt to remove thermal history.

The microphase-separated structure was identified using atom force microscopy (AFM). The AFM experiments were performed on a FemtoScan instrument. The films were obtained by a spin-coating method from the THF solution (25 mg mL^{-1}) of the triblock copolymer on glass substrates. After the solvent was removed at room temperature, the films were first annealed to 135 °C which was above the clearing point of the LC phase, and then slowly cooled to room temperature.

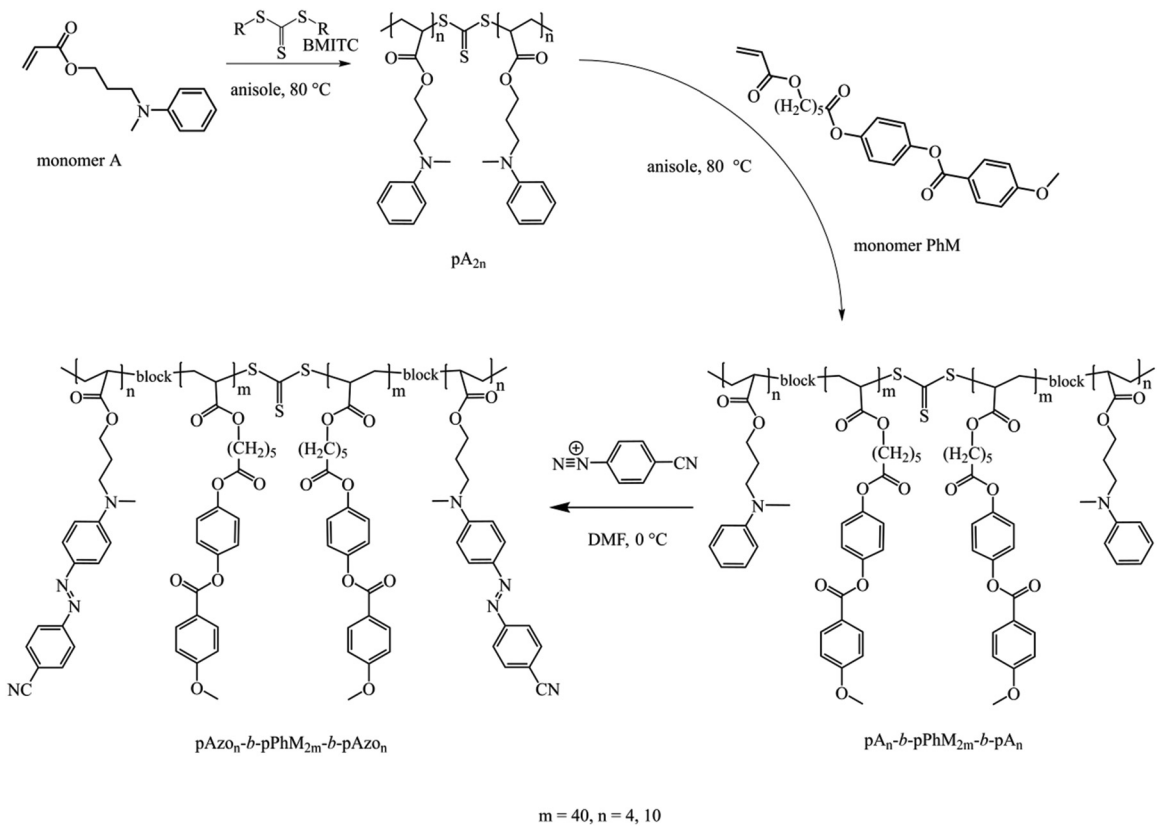

Scheme 1 General synthetic route for the azobenzene-containing fully LC symmetrical triblock copolymer.

In situ WAXS/SAXS experiments were performed using a Xenocs WAXS/SAXS machine equipped with a GeniX3D generator (l = 1.54 Å) producing an X-ray beam of approximately 300 × 300 μm^2 size. A Rayonix LX-170HS detector was used for WAXS data collection at a sample-to-detector distance of 20 cm. For SAXS data collection, a Pilatus 300k detector was employed. The norm of the reciprocal space vector **s** ($|\mathbf{s}|$ = 2 sin θ/λ, where θ is the Bragg angle and λ the wavelength) was calibrated using seven orders of Ag behenate for the WAXS region and three orders for the SAXS region. For data reduction and analysis, home-made programs designed in Igor Pro (Wavemetrics Ltd) were used.

For photooptical experiments, thin polymer films were obtained by spin-coating from solutions of different concentrations in THF. In order to completely remove any traces of THF the spin-coated films were kept at room temperature for one day. The films were about 400 nm for homopolymers and 1.5 μm for copolymers. Measurements were carried out with a profilometer.

Photochemical investigations were performed using an optical setup equipped with a DRSh-250 ultra-high pressure mercury lamp. Light with wavelength 404, 436 or 546 nm was selected using an interference filter. To prevent the heating of the samples due to IR irradiation of the lamp, a water filter was used. The intensity of light was measured using a Laser-Mate-Q (Coherent) intensity meter.

Spectral measurements were performed using a Unicam UV-500 UV-Vis spectrophotometer. The ratio of *E*- and *Z* isomers in the photostationary state of azobenzene-containing polymers in solutions and as-casted amorphous films was estimated by Fisher's method.[62] The linearly polarized spectra of the film samples were studied with a TIDAS spectrometer (J&M) equipped with a rotating polarizer (a Glan-Taylor prism controlled by a computer program).

The dichroism values, D, of the polymer films were calculated from the spectra using the following equation:

$$D = \frac{A_{\perp} - A_{||}}{A_{\perp} + A_{||}} \quad (1)$$

where $A_{||}$ and $A_{\perp}$ are the optical absorptions at 422 nm or 260 nm measured with light linearly polarized in the direction parallel and perpendicular to the polarization of the exciting 546 nm light, respectively.

Results and discussion

Homo- and block copolymer synthesis

For the synthesis of triblock copolymers and random copolymers the combination of RAFT polymerization which was employed advantageously to synthesize symmetric acrylic triblock copolymers containing optically active cholesterol mesogenic groups[63] and a post-polymerization azo-coupling reaction described in ref. 61 have been used (Scheme 1). Aiming at the controlled synthesis of LC symmetrical triblock copolymers we have applied RAFT polymerization using bifunctional symmetrical trithiocarbonate BMITC; the latter has already been successfully used for the RAFT polymerization of various vinyl monomers (*e.g.*, acrylates, styrene, vinyl acetate, and acrylonitrile).[64]

The reversible chain transfer reactions occurring in the polymerization mediated by symmetric trithiocarbonates are as follows:

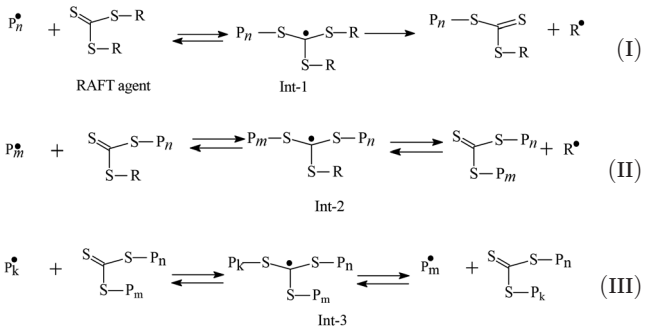

According to this mechanism, the "revival" of propagating radicals is provided by the multiple repetitions of reactions (II) and (III). Depending on the predominant way of chain "revival," the position of the trithiocarbonate group in a chain may differ.

If reaction (II) prevails, this group is located at the chain end; if reaction (III) predominates, this group sits within the chain. At a relatively low degree of polymerization, the position of the trithiocarbonate group may affect the properties of the polymer.

However, it is well known that in conventional free-radical polymerization of acrylic monomers, the transfer reaction of propagating macroradicals to the azobenzene fragment occurs.[65] Our preliminary experiments revealed poor control over the molecular mass characteristics of poly(3-[(4-[(4-cyanophenyl)diazenyl]phenyl)(methyl)-amino]propyl acrylate) in the presence of series of RAFT agents. This fact impelled us to use another strategy and the desired triblock copolymers were obtained (*cf.* Scheme 1) in three steps: (1) trithiocarbonate-mediated polymerization of monomer A, (2) block copolymerization of the monomer PhM in the presence of the resultant polymeric trithiocarbonate pA$_n$, and (3) the subsequent chemical modification of the resultant block copolymer *via* Azo-coupling reaction.

The first experiments revealed BMITC to be the more efficient RAFT agent among other representatives of trithiocarbonates.[58] The addition of 0.1 mol L^{-1} of BMITC to the polymerization of monomer A initiated by AIBN (10^{-3} mol L^{-1}) led to the formation of an oligomeric product, whose number average molecular mass M_n increased with the progress in monomer conversion (Table S1†) and was sufficiently close to the theoretical value:

$$M_n = \frac{q[M]_0}{[BMITC]_0 + 2f[AIBN]_0 e^{-k_i t}} \quad (2)$$

where q is monomer conversion, $[M]_0$, $[BMITC]_0$, and $[AIBN]_0$ – molar concentrations of the monomer A, RAFT agent and

initiator, respectively, f – initiator efficiency, k_i – initiation rate coefficient, and t – polymerization time.[66]

The polymerization in this case proceeded relatively rapidly: limited conversions were reached during 2 h of heating at 80 °C. However the PDI value slightly increased in the course of the polymerization, which under conditions of hundredfold molar excess of RAFT agent to the initiator might be caused by the side reaction of the substituted amino group of the monomer and the propagating radical.[67] The fact that PDI remains much lower than that of the polymers synthesized *via* conventional free radical polymerization indicates that most of the polymeric chains are formed *via* reactions (I)–(III).

The chain extension confirms more reliably the living nature of the process. Hence two polymers pA_{2n} where n = 4, 10 (see the Experimental section) containing an active trithiocarbonate moiety have been used in solution polymerization of monomer PhM (1 mol L^{-1}) as polymeric RAFT agents. In this case the formation of symmetrical triblock copolymers pA_n-*b*-$pPhM_m$-*b*-pA_n is expected, where the incorporation of monomer PhM units into the polymeric chain occurs between the sulfur atom of the trithiocarbonate group and the terminal unit of polymeric substituents (see Scheme 1). It is necessary to note that as we have shown previously, the trithiocarbonate group in initial homopolymer RAFT agents pA_{2n} is located virtually in the middle of the chain[58] and the structure of polymeric RAFT agents may be presented as pA_n–S–C(=S)–S–pA_n.

As can be seen from Table 1, the molecular mass distributions of the block copolymers are wider (polydispersity indexes of ~1.5) than those of initial polymers. Note that, in the RAFT polymerization of acrylic monomers in solution, a decrease in the monomer concentration usually leads to the same effect.[68] On the whole, it may be stated that pA_{2n} were efficient RAFT agents in the polymerization of monomer PhM and all block copolymers are enriched in monomer PhM units (Table 1). The chemical modification of the obtained block copolymers was conducted by the azocoupling reaction, in which a proton in the aromatic ring located in the *para*-position with respect to the nitrogen atom is replaced by an Azo group. The degree of conversion was quantified from the ^{1}H NMR data (Fig. 2). After chemical modification, the integral intensity of the peak at ~6.7 ppm corresponding initially to three protons of the aromatic ring decreased due to the reduction of the amount of protons owing to replacement of protons situated in the *para*-position with respect to the amino group with an azo group during modification. Moreover, the chemical shift of protons located at the *meta*-position with respect to the amino group changes from ~7.1 ppm to ~7.7 ppm. This effect is associated with the strong electron-acceptor properties of the incorporated fragment. Also the ratio of integral intensities of the peaks at ~7.7 ppm and 6.7 ppm is equal to three that corresponds to the ratio of the numbers of non-equal protons in the azobenzene group. The above data indicated that the degree of substitution is close to 100%, and the desired triblock copolymers containing nematogenic phenyl benzoate and photosensitive azobenzene groups have been successfully synthesized. Note that there is no change in the polydispersity index before and after the post-polymerization modification. The molecular characteristics of all the synthesized polymers estimated from data of GPC and ^{1}H NMR spectroscopy are given in Table 1.

Phase behavior

The phase behavior of the synthesized polymers was investigated by a combination of differential scanning calorimetry (DSC), thermal polarized microscopy (POM) and X-ray scattering. The phase transition temperatures of all samples were obtained from the first cooling (Fig. S8 and S9†) and second heating scans; the results are summarized in Table 2. DSC curves of the homopolymers are given in Fig. 3. Homopolymers pA_{20} and pA_8 are amorphous and are characterized by a low glass transition temperature (T_g) close to – 28 °C and −25 °C respectively. After the post-polymerization Azo-coupling reaction the phase behavior of the homopolymers is sharply changed: $pAzo_{20}$ has a higher T_g of 75 °C and its DSC curve shows only one transition temperature at 155 °C (Fig. 3).

In this temperature range the fan-shaped birefringent texture specific to smectic A (SmA) phase is observed (*cf.* the

Table 1 Molecular weights and distributions of the macromolecular chain transfer agents (homopolymers), triblock copolymers, and random copolymers obtained from GPC with calibrated polystyrene standards and ^{1}H NMR

Polymers	M_w/M_n	DP (A_n) or (Azo_n)[a]		Molar fraction of block PhM[b]	DP (PhM_n)	
		GPC	^{1}H NMR		GPC	^{1}H NMR
pA_8	1.17	8	6	0	0	0
pA_{20}	1.36	20	19	0	0	0
pA_4-*b*-$pPhM_{80}$-*b*-pA_4	1.55	8	6	0.9	80	70
pA_{10}-*b*-$pPhM_{80}$-*b*-pA_{10}	1.52	20	19	0.8	80	80
pA_7-*ran*-$pPhM_{30}$	1.35	7	9	0.8	30	40
$pAzo_{20}$	1.39	20	19	0	0	0
$pAzo_4$-*b*-$pPhM_{80}$-*b*-$pAzo_4$	1.55	8	6	0.9	80	70
$pAzo_{10}$-*b*-$pPhM_{80}$-*b*-$pAzo_{10}$	1.52	20	19	0.8	80	80
$pAzo_7$-*ran*-$pPhM_{30}$	1.41	7	9	0.8	30	40

[a] DP – degree polymerization. [b] Determined by ^{1}H NMR spectroscopy.

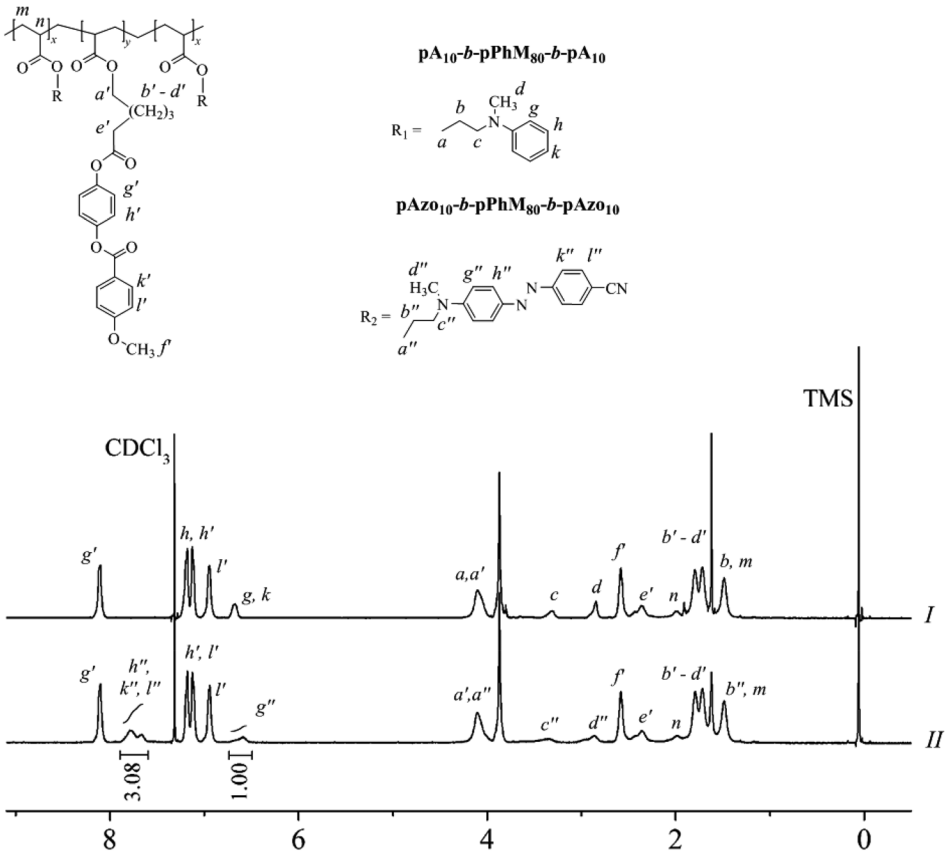

Fig. 2 ^{1}H NMR spectra of block copolymers (I) pA_{10}-*b*-$pPhM_{80}$-*b*-pA_{10} and (II) $pAzo_{10}$-*b*-$pPhM_{80}$-*b*-$pAzo_{10}$.

Table 2 Thermal transition data and mesomorphic properties for the homopolymers, block and random copolymers prepared by RAFT and obtained from the second heating scans

Polymers[a]	T_g, °C	Phase behaviour[b] (second heating), °C
$pPhM_{80}$	25	N 125 (0.9) I
$pAzo_{20}$	75	SmA 155 (2.2) I
pA_4-*b*-$pPhM_{80}$-*b*-pA_4	29	N 119 (0.8) I
pA_{10}-*b*-$pPhM_{80}$-*b*-pA_{10}	−1/28	N 122 (0.9) I
$pAzo_4$-*b*-$pPhM_{80}$-*b*-$pAzo_4$	33	N 122 (0.9)I
$pAzo_{10}$-*b*-$pPhM_{80}$-*b*-$pAzo_{10}$	33	LC 136 (1.4) I
pA_7-*ran*-$pPhM_{30}$	21	N 75 (0.7) I
$pAzo_7$-*ran*-$pPhM_{30}$	37	N 108 (0.7) I

[a] Subscripts indicate the polymerization degree of subblocks. [b] Mesophases: N is the nematic phase, SmA is the smectic phase A, and I is the isotropic melt. Isotropization enthalpy (in J g^{-1}) is given in brackets.

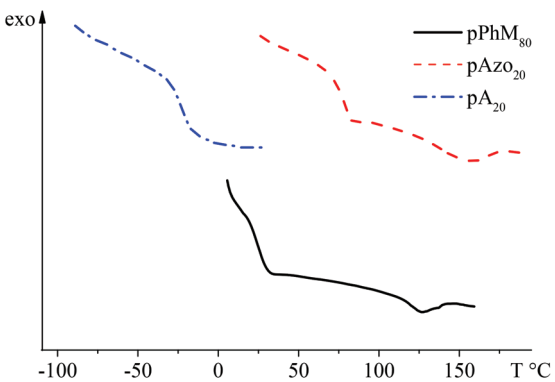

Fig. 3 DSC curves of the homopolymers pA_{20}, $pAzo_{20}$ and $pPhM_{80}$ obtained from the second heating scans.

microphoto in polarized light in Fig. S10a†). The homopolymer $pAzo_8$ has the same T_g as $pAzo_{20}$.

To probe the structure of the Azo-containing homopolymers, X-ray scattering experiments were performed on uniaxially-aligned samples of $pAzo_{20}$ at room temperature. The samples were drawn from the polymer melt. Fig. 4a and b show diffraction patterns acquired on the fiber sample of $pAzo_{20}$. They display three sharp peaks positioned at 24.51, 12.27 and 8.17 Å and oriented along the equatorial direction on the pattern. Such peaks with a ratio of *d*-spacings of 1 : 2 : 3 indicate that the $pAzo_{20}$ homopolymer forms a SmA phase. In the wide-angle region, a diffuse diffraction peak corresponding to an average interatomic distance of 4.32 Å is visible. This peak likely corresponds to a disordered arrangement of the mesogenic groups within the smectic layers parallel to the fiber axis.

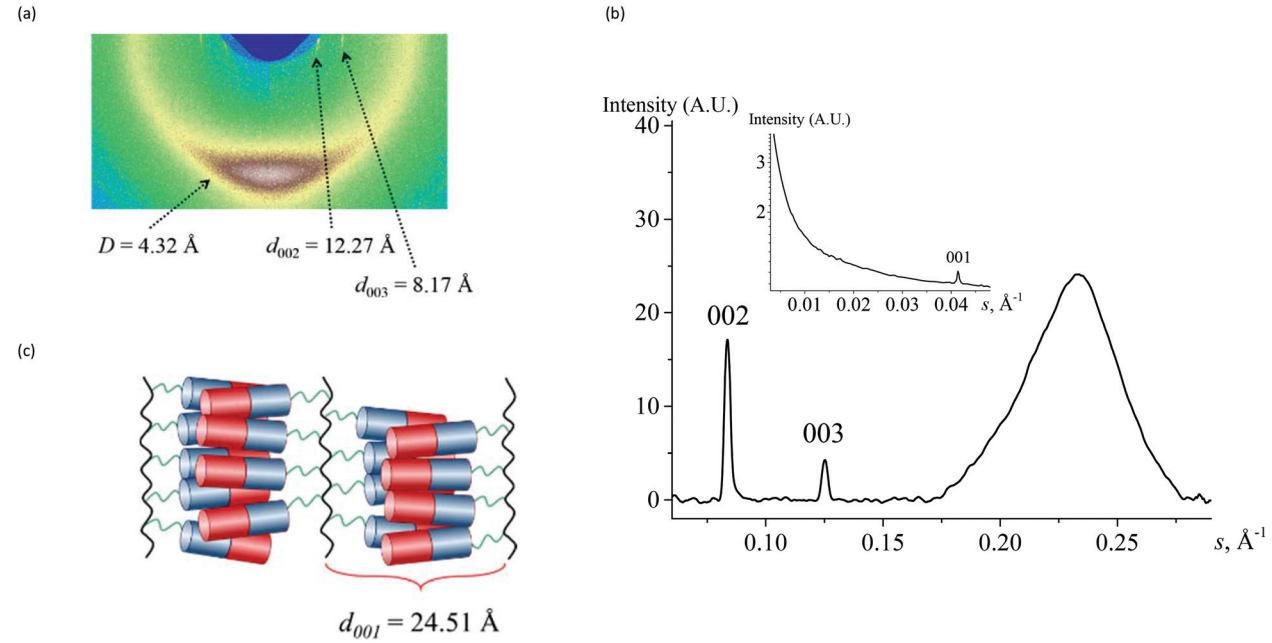

Fig. 4 (a) 2D WAXS pattern corresponding to the fiber sample of $pAzo_{20}$, (b) 1D WAXS and SAXS (inset) diffractograms of $pAzo_{20}$, and (c) scheme of the side-group arrangement in the SmA phase of the homopolymer $pAzo_{20}$ (the fiber axis is vertical).

From the fit of the three orders of the fundamental smectic peak to a linear law, the smectic layer thickness at 25 °C is estimated to be 24.51 Å. As the fully extended length of the Azo-containing monomer unit is calculated to be 21.19 Å, the side chains of the polymer are arranged according to the packing mode with fully interdigitated Azo-mesogens as depicted in Fig. 4c.

According to POM data (Fig. S10b†) only a marble texture was observed for $pPhM_{80}$. The DSC curves of the $pPhM_{80}$ homopolymer sample showed one endothermic peak at 125 °C (Fig. 3); the peak can be assigned to a nematic (N)–isotropic (I) phase transition, as was shown in our previous studies.[67] In addition, the glass transition temperature of the homopolymer was observed at around 25 °C.

Summarizing the phase behavior of the two triblock copolymers, *i.e.* pA_4-*b*-$pPhM_{80}$-*b*-pA_4 and $pAzo_4$-*b*-$pPhM_{80}$-*b*-$pAzo_4$, it can be noted that both of them have mesophase transitions from N to I phase between 119 and 122 °C (Table 2). The presence of nematic mesophase was confirmed by POM (Fig. S10c†) and X-ray data (not shown here). In this case, X-ray scattering in the wide-angle region displays only a diffuse maximum positioned at 4.35 Å. Importantly, all block copolymers are characterized by a single glass transition temperature independent of their composition.

As can be seen from Table 2, the N–I phase transition temperatures of the block copolymers (with the exception of $pAzo_{10}$-*b*-$pPhM_{80}$-*b*-$pAzo_{10}$) are slightly lower than those of the $pPhM_{80}$ homopolymer, forming a central subblock in the block copolymer. This means that the low content of pA and pAzo subblocks has no significant influence on the phase behavior of LC triblock copolymers, which is mainly determined by the $pPhM_{80}$ subblock. Therefore the pA and pAzo subblocks simply play the role of defects destabilizing the N phase. In contrast, the other two block copolymers, *i.e.* pA_{10}-*b*-$pPhM_{80}$-*b*-pA_{10} and $pAzo_{10}$-*b*-$pPhM_{80}$-*b*-$pAzo_{10}$, with a longer subblock of pA and pAzo show a different behavior. In POM (Fig. S10d†), the pA_{10}-*b*-$pPhM_{80}$-*b*-pA_{10} copolymer exhibits nematic mesophase typical of the pPhM block; it displays only one diffuse peak in WAXS. The DSC curves of the block copolymers are shown in Fig. 5.

Two T_g values were determined for the block copolymer pA_{10}-*b*-$pPhM_{80}$-*b*-pA_{10} (Table 2) which implies a phase separation between the subblocks. The first glass transition temperature occurs at around −1 °C, whereas the second one is

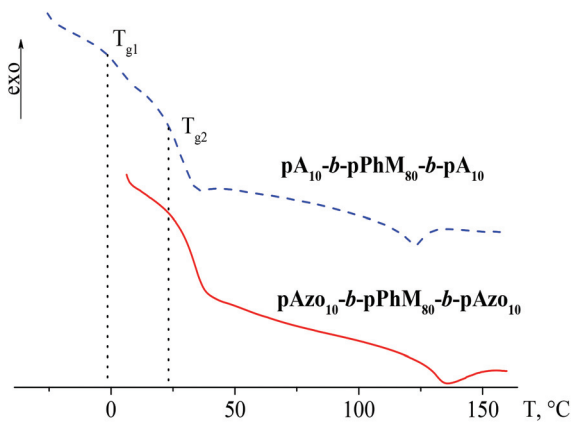

Fig. 5 DSC curves of the block copolymers obtained from the second heating scans.

pertinent to T_g of the $pPhM_{80}$ homopolymer. The result shows that introduction of the second subblock $pPhM_{80}$ into the macromolecule can dramatically increase the glass transition temperature of the pA subblock.

The $pAzo_{10}$-*b*-$pPhM_{80}$-*b*-$pAzo_{10}$ block copolymer also shows a nematic mesophase, according to POM (Fig. S10e†), and T_g around 33 °C, according to DSC measurements. The isotropization temperature of the block copolymer is higher after the formation of the Azo chromophores. Interestingly, this triblock copolymer exhibits an X-ray pattern similar to that of $pAzo_{20}$. The pattern displays three sharp scattering peaks at low angles (*cf.* Fig. 6), which correspond to the smectic phase and a diffuse wide-angle peak. The latter can belong to both the smectic and nematic phases, as the corresponding *d*-spacings are very close. It is noteworthy that we were not able to observe the microphase segregation mentioned above because the instrumental limit for the experimental setup used was around 70 Å. Importantly, although the random copolymer $pAzo_7$-*ran*-$pPhM_{30}$ has an identical percentage of the Azo groups as the block copolymer, it forms only a nematic mesophase (*i.e.*, the small-angle reflections are absent from the SAXS profiles; Fig. S10f and S11†). The comparison of the WAXS patterns corresponding to the fiber samples of the $pAzo_{20}$ homopolymer and the $pAzo_{10}$-*b*-$pPhM_{80}$-*b*-$pAzo_{10}$ block copolymer shows a different orientation of the side-chain layers with respect to the fiber axis (Fig. 4 and 6). In the latter case, the layers are oriented perpendicular to the long axis of the fiber unlike the homopolymer $pAzo_{20}$ (*cf.* the text above). To explain this, one can recall that the uniaxial orientation of polymers from the nematic mesophase is accompanied by the arrangement of the mesogenic side-groups parallel to the fiber axis, whereas the orientation of smectic SmA polymers results in disposition of smectic layers parallel to the direction of the mechanical field.[69]

In the block copolymer $pAzo_{10}$-*b*-$pPhM_{80}$-*b*-$pAzo_{10}$ the length of the block $pPhM_{80}$ forming the nematic mesophase is eight times larger than the length of the block $pAzo_{10}$ exhibiting the order of the Azo groups in the smectic layers. It can be

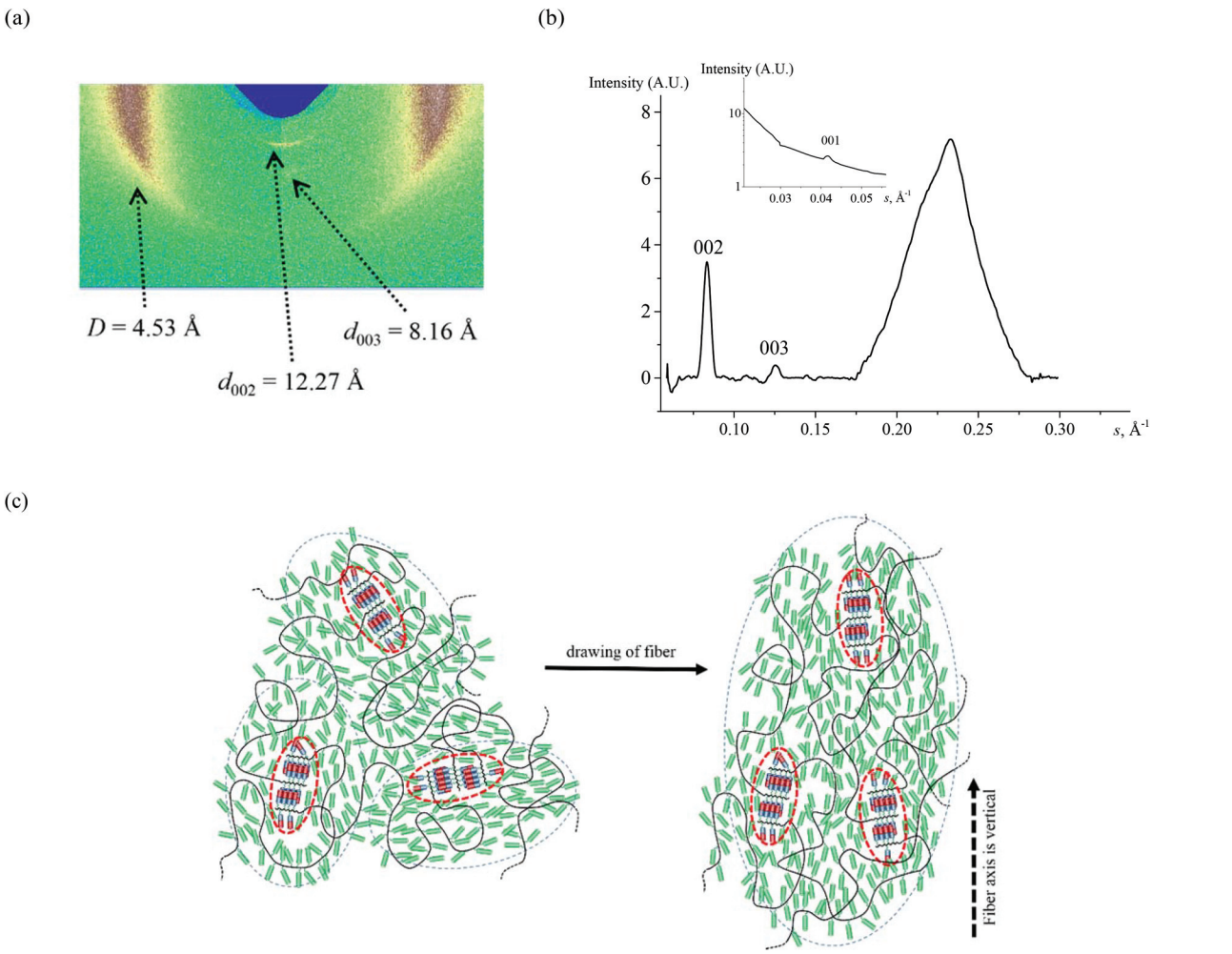

Fig. 6 (a) 2D WAXS pattern and (b) 1D WAXS and SAXS (in the inset) diffractograms corresponding to $pAzo_{10}$-*b*-$pPhM_{80}$-*b*-$pAzo_{10}$. (The fiber axis is vertical. The measurement was carried out at room temperature.) (c) Schematic representation of different mesogenic group orientations during uniaxial alignment of the block copolymer $pAzo_{10}$-*b*-$pPhM_{80}$-*b*-$pAzo_{10}$. The dashed line represents hypothetical domain boundaries.

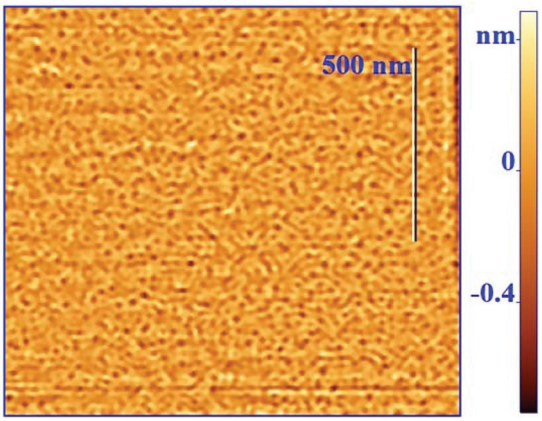

Fig. 7 AFM tapping mode height image for the annealed sample of $pAzo_{10}$-*b*-$pPhM_{80}$-*b*-$pAzo_{10}$.

assumed that the PhM groups make the main contribution to the orientation process, aligning along the drawing axis. As a result, the smectic layers formed by Azo groups become oriented perpendicular to the fiber axis. Schematically, the described process is represented in Fig. 6c. The results on orientation indirectly indicate that a microphase separation is present in the $pAzo_{10}$-*b*-$pPhM_{80}$-*b*-$pAzo_{10}$ block copolymer.

Moreover, the microphase-separated morphology of the block copolymer is revealed by AFM through the height images of free surfaces (Fig. 7) where the microphase-separated domain structure can be identified in the annealed films.

It is well-known that BCPs self-assemble into a range of different nanostructures, whose size can be controlled by the chain length, chemical functionality, volume fraction and the order of succession of each block.[70,71] In the $pAzo_{10}$-*b*-$pPhM_{80}$-*b*-$pAzo_{10}$ block copolymer the pAzo subblocks form separated phases: it was counted from AFM images (Fig. 7) that a share of the space occupied by domains (21%) approximately corresponds to the contents of the Azo-groups in the triblock copolymer (20%). The minority subphase formed by the pAzo blocks appears as dark dots in the phase image. The size of the observed microdomains fluctuates within 10–15 nanometers. Hence, it is possible to conclude that the domains (cylindrical or spherical form) are formed by pAzo segments, and the continuous matrix consists of $pPhM_{80}$ subblocks. The Azo groups are ordered in smectic layers inside domains, whereas the surrounding matrix represents a nematic phase formed by the $pPhM_{80}$ subblocks.

Photoinduced processes in azobenzene-containing polymers

Photooptical and photoorientation phenomena in the photochromic polymers were studied in the dilute solutions and in the thin amorphous films obtained by spin-coating. This method allows thin homogeneous amorphous polymer films to be obtained if the glass transition temperature of polymers is higher than ambient temperature.

As has been discussed above, all the synthesized azobenzene-containing polymers are characterized by different LC phase behaviors. Taking into account this fact, the investigation of the amorphous films (in which all polymers under discussion are remaining in the same "forced" isotropic phase state) will allow us to obtain information concerning the influence of chromophores distribution along the macromolecular chain on photoinduced processes occurring in these polymers under the light action.

The plan of this section may be described as follows. First, we will consider the optical properties and the results of studying the photochemical transformations in solution and in amorphous (isotropic) film of azobenzene-containing polymers. Then we will discuss the features of the photoorientation processes occurring in the amorphous films of homopolymer, block and random copolymers under the action of linearly polarized visible light.

Spectral absorption data and *E*–*Z* photoisomerization processes in solutions and in thin spin-coated films of photosensitive polymers

Fig. 8 shows the typical UV-vis absorbance spectra of the homopolymer $pAzo_{20}$ and the block copolymer $pAzo_{10}$-*b*-$pPhM_{80}$-*b*-$pAzo_{10}$ in THF solution. Before irradiation (t = 0) the spectra showed a band centered at 442 nm corresponding to the thermodynamically stable *E*-isomer of the azobenzene chromophore and attributed to the π–π* and n–π* electronic transitions (the n–π* transition band is not seen in the spectrum because of overlapping with the π–π* band; it is clearly seen from Fig. 8). This is typical for the push–pull type Azo chromophores.[72] A strong peak at around 260 nm was observed in copolymers. This peak is attributed to the superposition of the azobenzene aromatic core Φ–Φ* electronic transition, π–π* and n–π* electronic transitions of phenylbenzoate

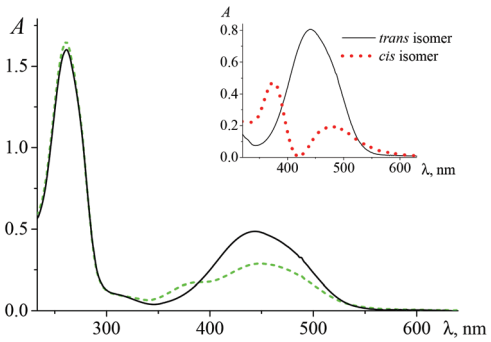

Fig. 8 UV-vis absorption spectra of the block copolymer $pAzo_{10}$-*b*-$pPhM_{80}$-*b*-$pAzo_{10}$ in THF solution before (solid line) and after illumination (for 3 min) in the photostationary state (dashed line). Irradiation conditions: room temperature, c = 1.8 × 10^{-5} M, λ = 436 nm, 1.5 mW cm^{-2}. The inset shows experimental absorbance spectrum of *E*-isomer of the homopolymer $pAzo_{20}$ in THF solution and the calculated spectral curve for its *Z*-isomer. The spectrum of the *Z* isomer was calculated from the two spectra in the photostationary state obtained for different λ_{ex} (404 and 436 nm) according to E. Fischer's method.[69]

chromophores. Let us mention that the maximum of the absorption spectra in the interval of the n–π* transition remains unchanged for all polymer solutions.

In contrast, the spectra of thin amorphous films of the homopolymer $pAzo_{20}$ and two block copolymers (Fig. 9a) are characterized by a hypsochromic shift of the π–π* absorption maximum centered between 425–438 nm depending on Azo group contents in comparison with their dilute solutions (λ_{max} = 442 nm).

Blue shift λ_{max} indicates that in the freshly prepared films based on these polymers, the formation of H-aggregates consisting of antiparallel packing of the azobenzene chromophores[72] is more strongly pronounced. Let us emphasize that equal degree of chromophore aggregation is observed in polymers $pAzo_{10}$-*b*-$pPhM_{80}$-*b*-$pAzo_{10}$ and $pAzo_{20}$ (their spectra coincide, Fig. 9a). The shift λ_{max} is less pronounced for $pAzo_4$-*b*-$pPhM_{80}$-*b*-$pAzo_4$, which indicates the smaller degree of aggregation in this copolymer (the π–π* absorption maximum centered at 438 nm).

At the same time, the dilution of azobenzene chromophores by phenylbenzoate groups in the random copolymer suppresses the aggregation process. The spectrum of thin films of the random copolymer $pAzo_7$-*ran*-$pPhM_{30}$ in which Azo moieties are uniformly distributed in the pPhM matrix practically coincides with its solution spectrum (the π–π* absorption maximum is centred at 444 nm). The position of this maximum corresponds apparently to nonassociated Azo-chromophores, in spite of the fact that the random copolymer contains the same percentage of Azo groups, similar to the block copolymer $pAzo_{10}$-*b*-$pPhM_{80}$-*b*-$pAzo_{10}$.

Irradiation of polymer solutions and films with the nonpolarized light (λ = 436 nm, I = 1.5 mW cm^{-2}) induces changes in absorption spectra of polymers which are typical for *E*–*Z* isomerization (Fig. 8 and 9b). It is clearly seen that an absorbance corresponding to the *E* isomer upon irradiation decreases and a photostationary state is achieved within 3 min. A slight increase of absorbance in the range of 382 nm also takes place. This absorbance increase is attributed to the n–π* electronic transition of the *Z*-isomer azobenzene chromophore whose content is increasing during the irradiation. Similar spectral features under the above mentioned conditions (λ = 436 nm, I = 1.5 mW cm^{-2}) were also observed for all the synthesized polymers with Azo-chromophores.

We have calculated according to E. Fischer's method[62] that polymer solutions in the photostationary state contain about 50% *Z*-isomer independently of the molecular architecture of macromolecules. In contrast, a considerably smaller concentration of *Z*-isomer is achieved in amorphous films of the polymer in the photostationary state (Table 3). The latter can be explained by the effects of the existence of the local free volume distribution in the polymer matrix and of the chain segmental mobility on the *E*–*Z* isomerization process.[73,74] The equally low *Z*-isomer content in $pAzo_{20}$ and $pAzo_{10}$-*b*-$pPhM_{80}$-*b*-$pAzo_{10}$ films is probably due, to a great part, to H-aggregates preventing the accumulation of *Z*-isomer in the photostationary state.

Meanwhile the content of *Z*-isomer is three times higher (Table 3) when the degree of aggregation is negligible ($pAzo_4$-*b*-pPhM-*b*-$pAzo_4$) or H-aggregates are absent ($pAzo_7$-*ran*-$pPhM_{30}$).

Table 3 *E*–*Z* isomer ratios in the photostationary state of azobenzene-containing polymers in solutions and in as-casted amorphous films after irradiation (λ = 436 nm, I = 1.5 mW cm^{-2})

	Z : *E*, %	
Polymers	Solution	Film
$pAzo_{20}$	51 : 49	13 : 87
$pAzo_{10}$-*b*-$pPhM_{80}$-*b*-$pAzo_{10}$	48 : 52	12 : 88
$pAzo_4$-*b*-pPhM-*b*-$pAzo_4$	50 : 50	35 : 65
$pAzo_7$-*ran*-$pPhM_{30}$	52 : 48	34 : 66

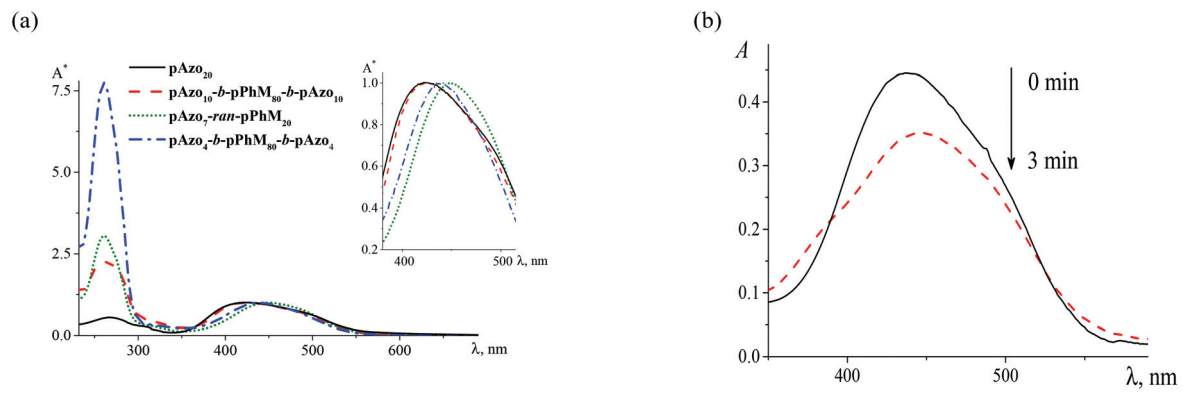

Fig. 9 (a) Absorbance spectra of as-casted amorphous homopolymer and copolymer films at room temperature normalized at a maximum of the π–π* electronic transition; the inset shows absorbance spectra of π–π* electronic transitions of Azo chromophores in detail (A^* = A/A_{max}, where A_{max} is the absorbance at a maximum of π–π* electronic transition of azo chromophores); (b) changes in absorbance spectra of $pAzo_{10}$-*b*-$pPhM_{80}$-*b*-$pAzo_{10}$ copolymer films after irradiation with nonpolarized light (λ = 436 nm, 1.5 mW cm^{-2}, 22 °C). The photostationary state of *E*–*Z* photoisomerization is achieved during 3 min.

Therefore, the distribution of chromophores along the macromolecular chain and their volume fraction have an essential influence on the aggregation phenomena and *E–Z* isomer ratios at the photostationary state in amorphous films of azobenzene-containing polymers.

Photoinduced optical anisotropy in spin-coated amorphous polymer films

It is well known that a majority of azobenzene-containing polymers undergo photoinduced orientational processes under illumination by polarized light. In our work, light induced optical anisotropy in polymer films has been studied by the investigation of the photogenerated dichroism using linearly polarized light (546 nm, 2 mW cm^{-2}). Preliminary investigations of the photooptical properties of amorphous polymer films of the synthesized azobenzene-containing polymers revealed that light exposure results in a preferred orientation of the azobenzene groups located perpendicular to the electric field vector of the linearly polarized light. As can be seen from Fig. 10, polarized light absorbance for all copolymers is noticeably higher for the polarization direction perpendicular to the polarization plane of the excitation light.

It is noteworthy that the values of maximum achievable dichroism of the azobenzene chromophore are the same (Fig. 10a, c and S12a†) for the homopolymer $pAzo_{20}$ and the block copolymer $pAzo_{10}$-*b*-$pPhM_{80}$-*b*-$pAzo_{10}$ in their amorphous films (D = 0.24), while for $pAzo_4$-*b*-$pPhM_{80}$-*b*-$pAzo_4$ the dichroism value is much smaller (D = 0.08, Fig. S12b†) according to the small concentration of the Azo groups. At the same time, among all the discussed copolymers, the $pAzo_7$-*ran*-$pPhM_{30}$, which contains the same percentage of Azo-groups as the block copolymer $pAzo_{10}$-*b*-$pPhM_{80}$-*b*-$pAzo_{10}$, is characterized by the maximum value of the induced dichroism (D = 0.57, Fig. 10b) among all the discussed copolymers. This dichroism value is in good agreement with the dichroism of the well-studied azobenzene containing side chain polymers.[24] Probably, an H-aggregation of photochromic groups in the homopolymer and block copolymers (Fig. 9a) studied by us partially hampers the photoorientation process, decreasing the achievable values of dichroism.

Kinetics curves of linear dichroism growth normalized to its maximum value are presented in Fig. 11. They clearly demonstrated the noticeable difference in the kinetics of dichroism growth for block and random copolymers. The obtained data revealed that initial rates of the azobenzene chromophore dichroism growth are almost the same for the homopolymer and all block copolymers: the dichroism value increases as a function of time and reaches a maximum during about 60–80 min. The copolymer $pAzo_7$-*ran*-PhM_{30} shows a completely different behavior: in the amorphous films the dichroism growth has slower evolution in such a way that 5 hours are needed to reach a maximum value.

Such a significant difference could be explained by the variation in the photoorientation process mechanism. Let us discuss these data in detail. As can be seen from Fig. 9a, the

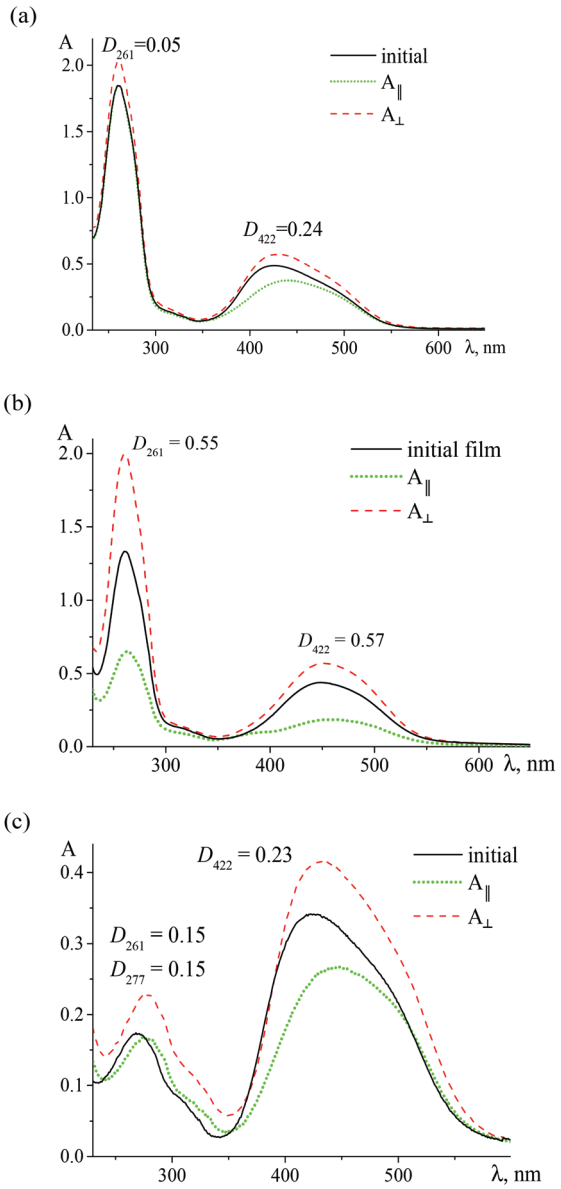

Fig. 10 Polarized absorbance spectra of the as-casted films $pAzo_{10}$-*b*-$pPhM_{80}$-*b*-$pAzo_{10}$ (a), $pAzo_7$-*ran*-$pPhM_{30}$ (b) and $pAzo_{20}$ (c) before (solid line) and after polarized light action (dash and dotted lines). Irradiation conditions: 546 nm, 2 mW cm^{-2}, 22 °C. Irradiation time is equal to 1 hour for $pAzo_{10}$-*b*-$pPhM_{80}$-*b*-$pAzo_{10}$ and $pAzo_{20}$ and 5 hours for $pAzo_7$-*ran*-$pPhM_{30}$.

E-azobenzene moieties have very small absorption in the vicinity of 260 nm, where absorption of the phenyl benzoate mesogenic groups is also observed. This absorption peak becomes more pronounced with decreasing the amount of Azo-groups with respect to $pPhM_{80}$ subblocks in copolymers (the contribution of Azo groups to the absorption peak is about 15%). Taking into account the slight absorption of Azo-groups at 260 nm, the dichroism values of phenyl benzoate mesogenic groups of copolymers have been calculated neglecting the Azo group absorption (Fig. 10).

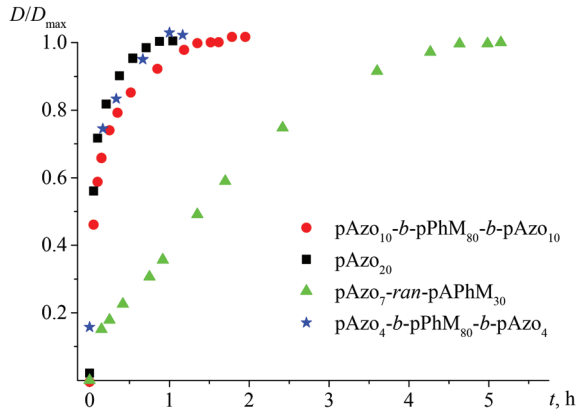

Fig. 11 Kinetics of the azobenzene chromophore dichroism (D) growth normalized to its maximum value (D_{max}) upon irradiation of polymer films with polarized light (546 nm, 2 mW cm^{-2}, 22 °C).

The dichroism values at 260 nm and 422 nm are practically identical for the homopolymer $pAzo_{20}$ and the block copolymer $pAzo_{10}$-*b*-$pPhM_{80}$-*b*-$pAzo_{10}$ (Fig. 10a and c). The small photoinduced dichroism in the film of $pAzo_{20}$ at 260 nm is associated with the orientation of Azo-groups. This result shows that practically only Azo groups are included in the process of photoinduced orientation in spin-coated amorphous films of the block copolymer $pAzo_{10}$-*b*-$pPhM_{80}$-*b*-$pAzo_{10}$. In other words the subblocks $pPhM_{80}$ do not participate in this process and do not prevent orientation of the pAzo subblocks.

In contrast, in the case of the random copolymer $pAzo_7$-*ran*-$pPhM_{30}$, the dichroism values at 260 nm and 422 nm are equal and significantly larger than those for the block copolymer $pAzo_{10}$-*b*-$pPhM_{80}$-*b*-$pAzo_{10}$. This means that the orientational cooperative effect of both the azobenzene chromophore and the phenyl benzoate mesogenic groups is observed. The same situation was usually observed for a majority of azobenzene copolymers described in the literature.[24]

Conclusions

A novel synthetic route that allows one to obtain symmetrical photosensitive fully liquid crystalline side chain triblock copolymers and random copolymers with nematogenic phenyl benzoate and photosensitive azobenzene containing mesogenic groups that combines RAFT polymerization and subsequent chemical modification has been developed. The results of the polymerization of acrylic monomer A with methylaniline groups proved that *S*,*S*′-bis(methyl-2-isobutyrate)trithiocarbonate is an effective RAFT agent. The ^{1}H NMR and chain extension results confirmed the RAFT process of such a polymerization. The central block of synthesized photochromic block copolymers contains 80 phenyl benzoate mesogenic groups (PhM), while the length of the "peripheral" blocks includes 4 or 10 azobenzene (Azo) units. Random copolymer with the same mesogenic units, "basic" homopolymers and block copolymers, containing methylaniline (A) groups, using an azocoupling reaction have been also synthesized as reference samples. The results demonstrated that microphase separation structure is observed in block copolymers when the length of the subblock with Azo and A groups reaches ten monomeric units. It was shown that the distribution of chromophores along the macromolecular chain and their volume fraction have an essential influence on the aggregation phenomena, isomerization ratios at the photostationary state and the mechanism of their photoorientation in amorphous films of Azo-containing polymers. The dichroism growth kinetics in amorphous copolymers films is studied and the influence of polymers molecular architecture on the photoinduced dichroism is revealed. This study shows that practically only Azo groups are included in the process of photoinduced orientation in spin-coated amorphous films of block copolymers, whereas the orientational cooperative effect of both azobenzene chromophore and phenyl benzoate mesogenic groups is observed only in the case of random copolymers.

Acknowledgements

This research was financially supported by the Russian Science Foundation (Grant No. 14-13-00379: synthesis of polymers, thermal behavior, and photochemical and photooptical studies, N.I. Boiko, M.A. Bugakov, A.A. Piryazev, V.P. Shibaev) and by the Russian Ministry of Science and Education (Project No. 11.G34.31.0055: X-ray analysis). The authors are grateful to Olga Sinitsyna for helpful discussions.

References

1 T. Ikeda and Y. Zhao, *Smart Light-Responsive Materials: Azobenzene Containing Polymers and Liquid Crystals*, John Wiley & Sons Inc., Hoboken, New Jersey, 2009.
2 H. Ringsdorf, H. W. Schmidt, H. Eilingsfeld and K. H. Etzbach, *Makromol. Chem.*, 1987, **188**, 1355–1366.
3 S. Hvilsted, F. Andruzzi, C. Kulinna, H. W. Siesler and P. S. Ramanujam, *Macromolecules*, 1995, **28**, 2172–2183.
4 B. Tylkowski, S. Peris, M. Giamberini, R. Garcia-Valls, J. A. Reina and J. C. Ronda, *Langmuir*, 2010, **26**, 14821–14829.
5 X. Pei, A. Fernandes, B. Mathy, X. Laloyaux, B. Nysten, O. Riant and A. M. Jonas, *Langmuir*, 2011, **27**, 9403–9412.
6 T. Ikeda, S. Horiuchi, D. B. Karanjit, S. Kurihara and S. Tazuke, *Macromolecules*, 1990, **23**, 42–48.
7 B. Zupancic, S. Diez-Berart, D. Finotello, O. D. Lavrentovich and B. Zalar, *Phys. Rev. Lett.*, 2012, **108**, 257801.
8 P. V. Dolganov, E. I. Demikhov, V. K. Dolganov, B. M. Bolotin and K. Krohn, *Eur. Phys. J. E*, 2003, **12**, 593–597.
9 S. K. Prasad, *Mol. Cryst. Liq. Cryst. Lett. Sect.*, 2009, **509**, 317–327.

10 H. Finkelmann, E. Nishikawa, G. G. Pereira and M. Warner, *Phys. Rev. Lett.*, 2001, **87**(1), 015501.
11 Y. L. Yu, M. Nakano and T. Ikeda, *Nature*, 2003, **425**(6954), 145.
12 M. H. Li, P. Keller, B. Li, X. G. Wang and M. Brunet, *Adv. Mater.*, 2003, **15**(7–8), 569–572.
13 A. Shimamura, A. Priimagi, J. Mamiya, T. Ikeda, Y. Yu, C. J. Barrett and A. Shishido, *Appl. Mater. Interfaces*, 2011, **3**, 4190–4196.
14 K. M. Lee, D. H. Wang, H. Koerner, R. A. Vaia, L. S. Tan and T. White, *Angew. Chem., Int. Ed.*, 2012, **51**, 4117–4121.
15 K. M. Lee and T. J. White, *Macromolecules*, 2012, **45**, 7163–7170.
16 K. M. Lee, N. V. Tabiryan, T. J. Bunning and T. J. White, *J. Mater. Chem.*, 2012, **22**, 691–698.
17 A. Ryabchun, A. Bobrovsky, J. Stumpe and V. Shibaev, *Macromol. Rapid Commun.*, 2012, **33**, 991–997.
18 D. Y. Kim, S. K. Tripathy, L. Li and J. Kumar, *Appl. Phys. Lett.*, 1995, **66**(10), 1166–1168.
19 P. Rochon, E. Batalla and A. Natansohn, *Appl. Phys. Lett.*, 1995, **66**(2), 136–138.
20 D. Kessler, F. D. Jochum, J. Choi, K. Char and P. Theato, *Appl. Mater. Interfaces*, 2011, **3**, 124–128.
21 F. Weigert, *Verh. Dtsch. Phys. Ges.*, 1919, **21**, 479.
22 M. Eich and J. H. Wendorff, *Makromol. Chem., Rapid Commun.*, 1987, **8**, 467–471.
23 V. Shibaev, *Polymers as Electrooptical and Photooptical Active Media*, Springer-Verlag, Berlin, Heidelberg, New York, 1996.
24 V. Shibaev, A. Bobrovsky and N. Boiko, *Prog. Polym. Sci.*, 2003, **28**(5), 729–836.
25 A. Natansohn and P. Rochon, *Chem. Rev.*, 2002, **102**(11), 4139–4175.
26 J. A. Delaire and K. Nakatani, *Chem. Rev.*, 2000, **100**(5), 1817–1845.
27 K. Ichimura, *Chem. Rev.*, 2000, **100**, 1847–1874.
28 M. J. Kim, S. J. Yoo and D. Y. Kim, *Adv. Funct. Mater.*, 2006, **16**, 2089–2094.
29 J. Kumar, L. Li, X. L. Jiang, D. Kim, T. S. Lee and S. Tripathy, *Appl. Phys. Lett.*, 1998, **72**, 2096–2098.
30 R. H. Berg, S. Hvilsted and P. S. Ramanujam, *Nature*, 1996, **383**(6600), 505–508.
31 S. J. Zilker, M. R. Huber, R. Bieringer and D. Haarer, *Appl. Phys. B*, 1999, **68**, 893–897.
32 F. Ercole, T. P. Davis and R. A. Evans, *Polym. Chem.*, 2010, **1**, 37–54.
33 S. Kadota, K. Aoki, S. Nagano and T. Seki, *J. Am. Chem. Soc.*, 2005, **127**, 8266–8267.
34 H. Yu, K. Okano, A. Shishido, T. Ikeda, K. Kamata, M. Komura and T. Iyoda, *Adv. Mater.*, 2005, **17**, 2184–2188.
35 K. Aoki, T. Iwata, S. Nagano and T. Seki, *Macromol. Chem. Phys.*, 2010, **211**, 2484–2489.
36 H. F. Yu, A. Shishido, T. Iyoda and T. Ikeda, *Macromol. Rapid Commun.*, 2007, **28**, 927–931.
37 C. Berges, I. r. Javakhishvili, S. Hvilsted, C. Sánchez and R. Alcalá, *Macromol. Chem. Phys.*, 2012, **213**, 2299–2310.
38 Y. Zhu, Y. Zhou, Z. Chen, R. Lin and X. Wang, *Polymer*, 2012, **53**, 3566–3576.
39 C. F. Huang, W. Chen, T. P. Russell, A. C. Balazs, F. C. Chang and K. Matyjaszewski, *Macromol. Chem. Phys.*, 2009, **210**, 1484–1492.
40 Q. Yan, D. Han and Y. Zhao, *Polym. Chem.*, 2013, **19**, 5026–5037.
41 J. Heo, Y. J. Kim, M. Seo, S. Shin and S. Y. Kim, *Chem. Commun.*, 2012, **48**, 3351–3353.
42 A. Bobrovsky, N. Boiko and V. Shibaev, *Polymer*, 2015, **56**, 263–270.
43 V. Shibaev and N. Boiko, in *Silicon-containing dendritic polymers*, ed. P. R. Dvornic and M. J. Owen, 237 Advances in Silicon Science 2, Springer Science, Business Media B.V., 2009.
44 S. Hernandez-Ainsa, R. Alcala, J. Barbera, M. Marcos, C. Sanchez and J. L. Serrano, *Macromolecules*, 2010, **43**, 2660–2663.
45 E. Blasco, M. Piñol and L. Oriol, *Macromol. Rapid Commun.*, 2014, **35**, 1090–1115.
46 R. Deloncle and A. M. Caminade, *J. Photochem. Photobiol., C*, 2010, **11**, 25–45.
47 Y. Morikawa, T. Kondo, S. Nagano and T. Seki, *Chem. Mater.*, 2007, **19**, 1540–1542.
48 S. Nagano, Y. Koizuka, T. Murase, M. Sano, Y. Shinohara, Y. Amemiya and T. Seki, *Angew. Chem., Int. Ed.*, 2012, **51**, 5884.
49 Y. Zhu and X. Wang, *Dyes Pigm.*, 2013, **97**, 222–229.
50 Y. Zhao, X. Tong and Y. Zhao, *Macromol. Rapid Commun.*, 2010, **31**, 986–990.
51 Y. Zhao, B. Qi, X. Tong and Y. Zhao, *Macromolecules*, 2008, **41**(11), 3823–3831.
52 A. Natansohn, P. Rochon, X. Meng, C. Barrett, T. Buffeteau, S. Bonenfantand and M. Pézolet, *Macromolecules*, 1998, **31**, 1155–1161.
53 A. Natansohn and P. Rochon, *Chem. Rev.*, 2002, **102**(11), 4139–4175.
54 T. Todorov, L. Nikolova and N. Tomova, *Appl. Opt.*, 1984, **23**(23), 4309–4312.
55 X. G. Wang, J. I. Chen, S. Marturunkakul, L. Li, J. Kumar and S. K. Tripathy, *Chem. Mater.*, 1997, **9**(1), 45–50.
56 X. G. Wang, J. Kumar, S. K. Tripathy, L. Li, J. I. Chen and S. Marturunkakul, *Macromolecules*, 1997, **30**(2), 219–225.
57 I. A. Budagovsky, A. S. Zolot'ko, T. E. Koval'skaya, M. P. Smayev, S. A. Shvetsov, N. I. Boiko, M. A. Bugakov and M. I. Barnik, *Bull. Lebedev. Phys. Inst.*, 2014, **41**(5), 135–139.
58 M. A. Bugakov, N. I. Boiko, E. V. Chernikova and V. P. Shibaev, *J. Polym. Sci., Part B: Polym. Phys.*, 2013, **55**(5–6), 294–303.
59 E. V. Chernikova, Z. A. Poteryaeva, S. S. Belyaev, I. E. Nifant'ev, A. V. Shlyakhtin, Y. u. V. Kostina, A. S. Cherevan', M. N. Efimov, G. N. Bondarenko and E. V. Sivtsov, *Polym. Sci., Part B: Polym. Phys.*, 2011, **53**, 391–395.
60 N. Boiko, V. Shibaev and M. Kozlovsky, *J. Polym. Sci., Part B: Polym. Phys.*, 2005, **43**, 2352–2360.
61 D. Wang, G. Ye and X. Wang, *Macromol. Rapid Commun.*, 2007, **28**, 2237–2243.

62 E. Fisher, *J. Phys. Chem.*, 1967, **71**(11), 3704–3706.
63 M. G. Ivanov, N. I. Boiko, E. V. Chernikova, R. Richardson, X. M. Zhu and V. P. Shibaev, *J. Polym. Sci., Part A: Polym. Chem.*, 2011, **53**, 633–644.
64 E. V. Chernikova, D. V. Vishnevetskii, E. S. Garina, A. V. Plutalova, E. A. Litmanovich, B. A. Korolev, A. V. Shlyakhtin, Y. V. Kostina and G. N. Bondarenko, *Polym. Sci., Part B: Polym. Phys.*, 2012, **54**, 127–141.
65 L. Manfred, H. Hallensleben and B. Weichart, *Polym. Bull.*, 1989, **22**, 557–563.
66 G. Moad, E. Rizzardo and S. H. Thang, *Polymer*, 2008, **49**, 1079–1131.
67 G. Odian, *Principles of Polymerization*, John Wiley & Sons Inc., New York, 2004.
68 G. Moad, E. Rizzardo and S. H. Thang, *Aust. J. Chem.*, 2006, **59**, 669–692.
69 Y. S. Freidzon, R. V. Talroze, N. I. Boiko, S. G. Kostromin, V. P. Shibaev and N. A. Plate, *Liq. Cryst.*, 1988, **3**(1), 127–132.
70 M. R. Bockstaller, R. A. Mickiewicz and E. L. Thomas, *Adv. Mater.*, 2005, **17**, 1331–1349.
71 G. H. Fredrickson, *Phys. Today*, 1999, **52**, 32–40.
72 F. L. Labarthet, S. Freiberg, C. H. Pellerin, M. Pézolet, A. Natansohn and P. Rochon, *Macromolecules*, 2000, **33**, 6815–6823.
73 C. D. Eisenbach, *Makromol. Chem.*, 1978, **179**, 2489–2506.
74 I. Mita, K. Horie and K. Hirao, *Macromolecules*, 1989, **22**, 558–563.